Controls on leaf water hydrogen and oxygen isotopes: A local investigation across seasons and altitude

Jinzhao Liu[a, b*], Chong Jiang[a], Huawu Wu[c], Li Guo[d], Haiwei Zhang[e], Ying Zhao[f]

[a] State Key Laboratory of Loess and Quaternary Geology, Center for Excellence in Quaternary Science and Global Change, Institute of Earth Environment, Chinese Academy of Sciences, Xi'an 710061, China

[b] National Observation and Research Station of Earth Critical Zone on the Loess Plateau of Shaanxi, Xi'an, 710061, China

[c] Key Laboratory of Watershed Geographic Sciences, Nanjing Institute of Geography and Limnology, Chinese Academy of Sciences, Nanjing 210008, China

[d] State Key Laboratory of Hydraulics and Mountain River Engineering & College of Water Resource and Hydropower, Sichuan University, 610065, Chengdu, China

[e] Institute of Global Environmental Change, Xi'an Jiaotong University, Xi'an, 710054, China

[f] College of resources and environmental engineering, Ludong University, 264025, Yantai, China

[*]Corresponding author's email: liujinzhao@ieecas.cn (J. Liu)

Abstract

The stable oxygen ($\delta^{18}O_{leaf}$) and hydrogen ($\delta^{2}H_{leaf}$) isotopes of leaf water act as a bridge

that connects the hydroclimate to plant-derived organic matter. However, it remains unclear whether the source water (i.e., twig water, soil water, and precipitation) or meteorological parameters (i.e., temperature, relative humidity, and precipitation) are the dominant controls on $\delta^{18}O_{leaf}$ and $\delta^{2}H_{leaf}$. Here, we reported a seasonal analysis of $\delta^{18}O_{leaf}$ and $\delta^{2}H_{leaf}$ together with isotopes from potential source waters and meteorological parameters along an elevation transect on the Chinese Loess Plateau. We found that $\delta^{2}H_{leaf}$ values were more closely correlated with source water isotopes than $\delta^{18}O_{leaf}$ values, whereas $\delta^{18}O_{leaf}$ and $\delta^{2}H_{leaf}$ values were similarly correlated with meteorological parameters along the elevation transect. Dual-isotope analysis showed that the $\delta^{18}O_{leaf}$ and $\delta^{2}H_{leaf}$ values were closely associated because of their similar altitudinal and seasonal responses, generating a well-defined isotope line relative to the local meteoric water line (LMWL). We also compared the measured $\delta^{18}O_{leaf}$ and $\delta^{2}H_{leaf}$ values with predicted values by the Craig-Gordon model and found no significant differences between them. We demonstrate that the first-order control on $\delta^{18}O_{leaf}$ and $\delta^{2}H_{leaf}$ values was the source water, and the second-order control was the enrichment associated with biochemical and environmental factors on the Loess Plateau.

Short Summary

What controls leaf water isotopes? We answered the question from two perspectives: respective and dual isotopes. On the one hand, the $\delta^{18}O$ and $\delta^{2}H$ values of leaf water responded to isotopes of potential source water (i.e., twig water, soil water, and precipitation) and meteorological parameters (i.e., temperature, RH, and precipitation)

differently. On the other hand, dual $\delta^{18}O$ and $\delta^{2}H$ values of leaf water yielded a significant linear relationship associated with altitude and seasonality.

Keywords: Leaf water, stable isotope, controls, seasonality, altitude

1 Introduction

The stable isotope compositions of oxygen and hydrogen ($\delta^{18}O$ and $\delta^{2}H$, respectively) are increasingly being used as powerful tracers to follow the path of water from its input as precipitation, movement through the soil, and ultimately to its release as soil evaporation and leaf transpiration (Penna and Meerveld, 2019). Leaf water transpiration plays a key role in regulating the water balance at scales ranging from catchment to global. Terrestrial plants can enrich heavier isotopes (^{2}H and ^{18}O) in leaf water via evaporative fractionation through the stoma (Helliker and Ehleinger, 2000; Liu et al., 2015; Cernusak et al., 2016), which is highly dependent on atmospheric conditions (e.g., temperature and relative humidity) and biophysiological processes (Farquhar et al., 2007; Kahmen et al., 2011; Cernusak et al., 2016). Subsequently, the isotopic signals from leaf water are integrated into plant organic matter, such as cellulose (e.g., Barbour, 2007; Lehman et al., 2017) and leaf wax (Liu et al., 2016, 2021), as powerful proxies used for paleoclimate reconstruction (Pagani et al., 2006; Schefuβ et al., 2011; Hepp et al., 2020). However, although leaf water isotopes are the fundamental parameters in ecohydrology and organic biosynthesis, an adequate understanding of controls of leaf water isotopes and the role of source water and hydroclimate in determining leaf water

isotopes is still lacking.

$\delta^{18}O_{leaf}$ and $\delta^{2}H_{leaf}$ values are influenced first by a plant's source water (mainly water taken up by roots from the soil; Cernusak et al., 2016; Barbour et al., 2017; Munksgaard et al., 2017), and second by the enrichment associated with transpiration (Munksgaard et al., 2017). Soil water for terrestrial plants generally originates from local precipitation, and precipitation isotopes vary spatially and temporally, being subject to controls including temperature, altitude, latitude, distance from the coast, and amount of precipitation (Bowen, 2010; Bowen and Good, 2015; Cernusak et al., 2016). More specifically, soil water isotopes are determined by a mixture of individual precipitation events with distinct isotopic signals and are also affected by evaporation, both of which lead to the development of isotopic gradients in soil water with depth (Allison et al., 1983; Liu et al., 2015). Many studies have shown that the $\delta^{18}O$ and $\delta^{2}H$ values of root/xylem water can be used to characterize the water sources used by plants (Rothfuss and Javaux, 2017; Wu et al., 2018; Wang et al., 2019; Amin et al., 2020; Zhao et al., 2020; Liu et al., 2021a). These studies rested substantially on the assumption that no isotopic fractionation of $\delta^{18}O$ and $\delta^{2}H$ values occurs during water uptake by plant roots (Dawson and Ehleringer, 1991; Ehleringer and Dawson, 1992; Chen et al., 2020), except in saline or xeric environments (Lin and Sternberg, 1993; Ellsworth and Williams, 2007). Some recent studies showed, however, that the occurrence of isotopic fractionation during root water uptake was probably more common than previously thought, especially with respect to $\delta^{2}H$ values (Zhao et al., 2016; Wang et al., 2017;

Barbeta et al., 2019; Poca et al., 2019; Liu et al., 2021a).

In addition to plant source water, leaf water is also isotopically enriched through the evaporative process during transpiration. The enrichment of ^{18}O and ^{2}H by leaf water transpiration can be predicted using the Craig-Gordon model (C-G model). This model was initially proposed to describe the evaporative enrichment of a freely evaporating water body (Craig and Gordon, 1965) and has been modified for plant leaves under steady-state conditions (Dongmann et al., 1974; Farquhar and Cernusak, 2005). However, the C-G model fails to explain the intra-leaf heterogeneity of $\delta^{18}O_{leaf}$ and $\delta^{2}H_{leaf}$ (Cernusak et al., 2016; Liu et al., 2021b), which is currently described using a two-pool model (Leaney et al., 1985; Song et al., 2015) and/or an advection-diffusion model, as the *Péclet* effect (Farquhar and Lloyd, 1993; Farquhar and Gan, 2003). Subsequently, more complicated models have been developed to cover non-steady-state conditions (Ogée et al., 2007). These models emphasize a mechanistic understanding of leaf water isotopic fractionation, but the relevant parameters cannot be strictly constrained or precisely monitored, which hinders the use of these models under natural conditions (Plavcová et al., 2018).

This study combined the effects of measured source water isotopes and C-G model-predicted transpiration on $\delta^{18}O_{leaf}$ and $\delta^{2}H_{leaf}$ values. Our objectives were to deepen the understanding of the controls on the $\delta^{18}O_{leaf}$ and $\delta^{2}H_{leaf}$ across different seasons. Based upon these objectives, we repeatedly sampled soils, twigs, and leaves in May, July, and

September (representing spring, summer, and autumn, respectively) from the same ten plots distributed along an elevation transect. Simultaneously, we obtained the relevant meteorological parameters (e.g., temperature, relative humidity, and precipitation) from sites close to the sampling plots along the transect and used these to predict the $\delta^{18}O_{leaf}$ and $\delta^{2}H_{leaf}$ values. The combined analysis of concurrent measurements of $\delta^{18}O$ and $\delta^{2}H$ values in soil water, twig water, and leaf water with the predicted $\delta^{18}O$ and $\delta^{2}H$ values of leaf water from the C-G model associated with the surrounding meteorological parameters will help to identify the factors that control $\delta^{18}O_{leaf}$ and $\delta^{2}H_{leaf}$ values. Furthermore, we performed an isotope-based line analysis of the dual $\delta^{18}O$ and $\delta^{2}H$ values of leaf water, associated with altitude and seasonality. This study will improve our understanding of the environmental signals preserved within the $\delta^{18}O$ and $\delta^{2}H$ values extracted from plant organic biomarkers associated with leaf water.

2. Materials and Methods

2.1 Study area

The Qinling Mountains form the dividing line between northern and southern China and mark the boundary between the watersheds of the Yellow and Yangtze Rivers. Mt. Taibai (Fig. 1; 33. 96 °N, 107.77 °E) rises to 3767 m above sea level (asl) and is the peak in the Qinling Mountains; it has a warm temperate ecosystem characterized by a rich diversity of flora and fauna. The mean annual temperature at the bottom of Mt. Taibai is 12.9°C, and the mean annual precipitation is 609.5 mm (Zhang and Liu, 2010). The climate, soil, and vegetation vary significantly along our slope transect, exhibiting

a remarkable vertical geo-ecological zonation (Fig. 1). The area contains a variety of climate zones: warm temperate (< 1300 m asl), temperate (1300 - 2600 m asl), cool temperate (2600 - 3350 m asl), and alpine (> 3350 m asl). The soil types vary from yellow loess soil at low elevations, spectacular rocky outcrops at middle elevations, and glacial remnants at high elevations. Vegetation along the transect is mainly coniferous and broadleaf forests and alpine and subalpine vegetation (Fig. 1; Liu, 2021). The dominant species range from *Quercus variabilis*, *Q. aliena*, *Betula albosinensis*, *B. utilis*, *Abies fargessi,* and *Larix chinensis* forests to *Rhododendron clementinae* and *R. concinnum* alpine (Supplementary table S1).

2.2 Sampling strategy

Plants and soils were sampled in May, July, and September 2020, and samples were collected from 10 plots (3 × 3 m) covering all of the vegetation zones along the northern slope of Mt. Taibai, extending from 608 to 3533 m asl (Fig. 1). Among the plots, six sites (i.e., sites 2, 3, 4, 5, 8, and 10; Fig. 1) were selected as being the closest to the weather stations along the elevation transect, and they were used in order to obtain the *in-situ* meteorological data for analysis. For the plants, one or two dominant deciduous and coniferous trees were chosen in each plot across the vegetation zone (Supplementary Table S1). Several large leaves and suberized twigs were collected for each species. Three to ten large leaves were chosen for sampling, and a small number were collected in broadleaf forests and a large number in coniferous forests, depending on leaf size. The leaf samples were conducted in the context of the intact leaves because of the likely isotopic gradients within a leaf (Helliker and Ehleringer, 2000; Liu et al.,

2016). Our sampling period was between 12 pm and 3 pm because maximum diurnal enrichment of the leaf water isotopic composition occurs during this part of the day (Romero and Feakins, 2011; Liu et al., 2021). The twigs were collected simultaneously by cutting suberized twigs, and all of the twigs were cut into samples that were 3-4 cm long. The leaf and twig samples were immediately placed into glass vials with screw caps and sealed with polyethylene parafilm. For the soils, three surface soil samples (less than 10 cm deep) were collected from around the sampled plants using a small metal scoop at each plot. All sampling plots were located on slopes far from rivers and surface water bodies, which ensured that the soil water in each plot was derived exclusively from precipitation. Although the surface soil layers were collected only as the representatives of soil water in this study, these samples could provide a relatively good source of water for the plants, as supported by a prior study conducted along the same elevation transect (Zhang and Liu, 2010). The soil samples were tightly sealed in a polyethylene zipper bag on site. All plant and soil samples were stored in a cool box (~ 4 °C) in the field and immediately transported to the laboratory. The altitude of each plot was determined using a handheld GPS unit with an error of ± 5 m.

2.3 Isotope analysis

The water in the plant and soil samples was extracted using an automatic cryogenic vacuum extraction system (LI-2100 Pro, LICA United Technology Limited, Beijing, China). The auto-extraction process was set for 3 hours, and the extraction rate of water from the samples was more than 98%. The isotopic composition of the soil water was measured using a Picarro L2130-I isotope water analyzer (Sunnyvale, CA, USA) at the

State Key Laboratory of Loess and Quaternary Geology, Institute of Earth Environment, Chinese Academy of Sciences. The analytical accuracies were ±0.1‰ for $\delta^{18}O$ and ±1‰ for $\delta^{2}H$. An isotope ratio mass spectrometer was coupled to a high-temperature conversion elemental analyzer (HT2000 EA-IRMS, Delta V Advantage; Thermo Fisher Scientific, Inc. USA) to take isotopic measurements of twig and leaf water at the Huake Precision Stable Isotope Laboratory on the campus of Tsinghua Shenzhen International Graduate School. The measurement precisions were ± 0.2‰ and ± 1‰ for $\delta^{18}O$ and $\delta^{2}H$, respectively. The isotopic composition of $\delta^{18}O$ and $\delta^{2}H$ is expressed as an isotopic ratio:

$$\delta_{sample}(‰) = \left(\frac{R_{sample} - R_{standard}}{R_{standard}}\right) \times 1000 \quad (1)$$

where δ_{sample} represents $\delta^{18}O$ or $\delta^{2}H$, and R_{sample} and $R_{standard}$ indicate the ratio of $^{18}O/^{16}O$ or $^{2}H/^{1}H$ of the sample and standard, respectively. The $\delta^{18}O$ and $\delta^{2}H$ values are reported relative to the Vienna mean standard ocean water (VSMOW). In addition, the mean monthly $\delta^{18}O$ and $\delta^{2}H$ values of precipitation were determined using the Online Isotope in Precipitation Calculator (Bowen and Revenaugh, 2003).

2.4 Modelling isotopes of leaf water

The C-G equation can be approximated as follows (Cernusak et al., 2022):

$$\delta_e = \delta_s + \varepsilon^+ + \varepsilon_k + (\delta_v - \delta_s - \varepsilon_k) \times \frac{e_a}{e_i} \quad (2)$$

where δ_e is the predicted $\delta^{18}O$ and $\delta^{2}H$ values at the evaporative sites within leaves, δ_s is the $\delta^{18}O$ and $\delta^{2}H$ values of source water (equivalent to twig water in our study), ε^+ is the equilibrium fractionation between liquid water and vapour, and ε_k is the kinetic fractionation during the diffusion of vapour through the stomata and the

boundary layer.

In our analysis, we calculated Δ_v (the enrichment of atmospheric vapour relative to source water) as $\Delta_v = (\delta_v - \delta_s)/(1 + \delta_s)$, and the values of Δ_v are often close to $-\varepsilon^+$ at the isotopic steady-state (Barbour, 2007; Cernusak et al., 2016); therefore, we can calculate δ_v as $\delta_v = -\varepsilon^+ + (1 - \varepsilon^+)\delta_s$. In addition, $\frac{e_a}{e_i}$ is the ratio of the water vapour pressure fraction in the air relative to that in the intercellular spaces and is equal to the relative humidity (RH) in the air at steady state (Cernusak et al., 2022). Thus, Equation (2) can be derived as

$$\delta_e = (1 - h)(\varepsilon^+ + \varepsilon_k) + (1 - \varepsilon^+ h)\delta_s \quad (3)$$

where δ_s represents the isotopic values of twig water, and h is the mean annual or monthly RH (MARH or MMRH) in this study. The equilibrium fractionation (ε^+) varies as a function of temperature (Bottinga and Craig, 1969) and can be equated to $\delta^{18}O$ and δ^2H, as follows (Majoube, 1971):

$$\varepsilon_o^+(‰) = \left[\exp\left(\frac{1.137}{(273+T)^2} \times 10^3 - \frac{0.4156}{273+T} - 2.0667 \times 10^{-3}\right) - 1\right] \times 1000 \quad (4)$$

$$\varepsilon_H^+(‰) = \left[\exp\left(\frac{24.844}{(273+T)^2} \times 10^3 - \frac{76.248}{273+T} + 52.612 \times 10^{-3}\right) - 1\right] \times 1000 \quad (5)$$

The kinetic fractionation (ε_k) can be calculated for $\delta^{18}O$ and δ^2H as (Farquhar et al., 2007; Cernusak et al., 2016):

$$\varepsilon_k^O(‰) = \frac{28r_s + 19r_b}{r_s + r_b} \quad (6)$$

$$\varepsilon_k^H(‰) = \frac{25r_s + 17r_b}{r_s + r_b} \quad (7)$$

where r_s and r_b are the resistances of the stomatal and boundary layers, respectively (i.e., the inverse of the conductance of the stomatal and boundary layers). Previous studies found stomatal and boundary layer conductance values of 0.49 and 2.85 mol m^-

^{2} s^{-1}, respectively (Cernusak et al., 2016; Munksgaard et al., 2017), resulting in ε_k^O and ε_k^H values of 26.7 and 23.8, respectively.

2.5 Statistical analysis

Statistical analysis (i.e., the mean, maximum and minimum values, as well as the standard deviation) of the isotopes extracted from the precipitation, soil, twig, and leaf samples was performed to define the range and distribution of the $\delta^{18}O$ and $\delta^{2}H$ values across the seasons. The Pearson correlation method was used to assess the correlations between the $\delta^{18}O$ and $\delta^{2}H$ values among the different water types (i.e., precipitation, soil water, twig water, and leaf water). Hierarchical cluster analysis was used to show the relationships among $\delta^{18}O_{leaf}$ and $\delta^{2}H_{leaf}$ values and potential source water isotopes ($\delta^{18}O$ and $\delta^{2}H$ values in precipitation, soil water, twig water, and leaf water), and meteorological parameters such as mean annual and monthly precipitation (MAP and MMP), mean annual and monthly temperature (MAT and MMT), and mean annual and monthly relative humidity (MARH and MMRH). A one-way analysis of variance (ANOVA) combined with a *post hoc* Tukey's least significant difference (LSD) test was performed to identify the significant differences in the isotopic compositions of precipitation, soil, twig, and leaf waters across the months. Comparisons of the relationships of $\delta^{18}O$ and $\delta^{2}H$ in the soil and leaf water were performed using covariance analysis (ANCOVA) to compare slopes across months. The structural equation model (SEM) was used to explain the respective effects of source waters (i.e., twig water, soil water, and precipitation) and meteorological parameters (i.e., temperature, precipitation, and RH) on $\delta^{18}O_{leaf}$ and $\delta^{2}H_{leaf}$ values. The validated SEMs

generated a good model fit, as indicated by a non-significant χ^2 test ($p > 0.05$), a high comparative fit index (CFI > 0.95), and a low root mean square error of approximation (RMSEA < 0.05). A special SEM was constructed based on the Mantel R values in AMOS (version 24.0.0). Moreover, we used the Hybrid Single-Particle Lagrangian Integrated Trajectory (HYSPLIT) model (Draxler and Rolph, 2003) to calculate air mass back-trajectory for the central site (34.13°N, 107.83°E, 2270 m asl) in the study area. These trajectories were initiated four times daily (at 00:00, 06:00, 12:00, and 18:00 UTC), and their air parcel was released at 2300 m asl for May, July, and September 2020 and moved backwards by winds for 120 h (5 days).

3. Results

3.1 Differing response of $\delta^{18}O$ and $\delta^{2}H$ values of leaf water

The measured $\delta^{18}O$ and $\delta^{2}H$ values of leaf water responded differently to source water isotopes (Fig. 2a) and meteorological parameters (Fig. 2b) across the seasons. The leaf water $\delta^{18}O$ and $\delta^{2}H$ values ($\delta^{18}O_{leaf}$ and $\delta^{2}H_{leaf}$) were clustered with those of the twig water ($\delta^{18}O_{twig}$ and $\delta^{2}H_{twig}$; Fig. 2a) and with MARH, MAT, and MMT (Fig. 2b). The $\delta^{2}H_{leaf}$ values were more closely correlated with isotopes of the potential source waters (e.g., twig water, soil water, and precipitation) than the $\delta^{18}O_{leaf}$ values in different months (Fig. 2a). In contrast, leaf water $\delta^{18}O$ and $\delta^{2}H$ values were correlated with meteorological parameters (Fig. 2b) throughout the study period. These correlations were more significant in summer (July) and autumn (September) than in spring (May).

265 3.2 Comparisons of measured and predicted $\delta^{18}O$ and $\delta^{2}H$ values of leaf water

266 The $\delta^{18}O_{leaf}$ and $\delta^{2}H_{leaf}$ values predicted by the C-G model were compared with the
267 measured $\delta^{18}O$ and $\delta^{2}H$ values across all three months (Fig. 3). The C-G models
268 explained 49% and 70% of the observed variations in the $\delta^{18}O_{leaf}$ and $\delta^{2}H_{leaf}$ values,
269 respectively (Fig. 3a, c). The slopes of the relationships for both $\delta^{18}O$ and $\delta^{2}H$ values
270 of leaf water were less than one, which suggests that part of the bulk leaf water is
271 derived from unenriched vein water. However, there were no significant differences in
272 $\delta^{18}O_{leaf}$ ($p = 0.54$; Fig. 3b) and $\delta^{2}H_{leaf}$ values ($p = 0.93$; Fig. 3d) between the C-G model
273 predicted values and the measured values.

274

275 3.3 Variations of $\delta^{18}O$ and $\delta^{2}H$ values of different waters with seasons and altitude

276 There was a significant correlation between $\delta^{18}O_{leaf}$ and $\delta^{2}H_{leaf}$ values ($R^2 = 0.81$, $p <$
277 0.01; Fig. 4), with significant clusters of $\delta^{18}O_{leaf}$ and $\delta^{2}H_{leaf}$ values across the months,
278 and values were higher in May, intermediate in July, and lower in September (Fig. 4).
279 Within each month, the $\delta^{18}O_{leaf}$ and $\delta^{2}H_{leaf}$ values were depleted in ^{2}H and ^{18}O at higher
280 altitudes relative to lower altitudes. Likewise, the potential types of source water (i.e.,
281 twig water, soil water, and precipitation) exhibited consistent variations across the
282 months, showing values that were relatively higher in May, intermediate in July, and
283 lower in September (Supplementary Fig. S1). The correlations between $\delta^{18}O$ and $\delta^{2}H$
284 values among the source waters were also significant (Supplementary Fig. S2).
285 Nevertheless, the slopes and coefficients of determination (R^2) between the $\delta^{18}O$ and
286 $\delta^{2}H$ values showed a decrease for precipitation, soil water, twig water, and leaf water

from the three sampling months, except for soil water in May (Supplementary Fig. S2). In addition, the ANCOVA showed no significant differences for the regression lines for precipitation (df = 0.47, $F = 2.49$, $p = 0.11 > 0.05$), twig water (df = 53.2, $F = 0.42$, $p = 0.66 > 0.05$), and leaf water (df = 437.3, $F = 2.78$, $p = 0.08 > 0.05$) across study months but a significant difference for soil water across the months (df = 308.8, $F = 10.9$, $p < 0.05$).

4. Discussion

4.1 $\delta^{18}O$ and $\delta^{2}H$ values of leaf water

A recent global meta-analysis indicated that $\delta^{18}O_{leaf}$ and $\delta^{2}H_{leaf}$ values reflect environmental drivers differently and showed that $\delta^{2}H_{leaf}$ values more strongly reflect xylem water and atmospheric vapour $\delta^{2}H$ values, whereas $\delta^{18}O_{leaf}$ values more strongly reflect air relative humidity (Cernusak et al., 2022). Seasonal and localized observations along an elevation transect on the Chinese Loess Plateau supported these different responses of $\delta^{18}O_{leaf}$ and $\delta^{2}H_{leaf}$ to the isotopic composition of the source water and meteorological conditions (Fig. 2). This is likely due to the variation in precipitation isotopic values compared with that in leaf water evaporative enrichment is larger for $\delta^{2}H_{leaf}$ than $\delta^{18}O_{leaf}$ (Cernusak et al., 2022). In addition, we found stronger correlations between $\delta^{2}H_{leaf}$ and isotope values of the source water (twig water, soil water, and precipitation) than between $\delta^{18}O_{leaf}$ values and the source water isotope values (Fig. 2a). This is consistent with the global meta-analysis results (Cernusak et al., 2022). However, our localized study did not show a significantly different response of $\delta^{18}O_{leaf}$ and $\delta^{2}H_{leaf}$

values to meteorological parameters, which responded at almost equivalent magnitudes (Fig. 2b). These observations suggest that plant organic isotopic proxies such as leaf wax (Sachse et al., 2012; Liu et al., 2016) and cellulose (Barbour, 2007; Lehman et al., 2017), which originate from $\delta^{18}O_{leaf}$ and $\delta^{2}H_{leaf}$ values, can provide comparative information that indicates climatic signals (e.g., temperature, RH, and precipitation) in natural archives. These results argued with the recent global meta-analysis that $\delta^{18}O_{leaf}$ and $\delta^{2}H_{leaf}$ values reflect climatic parameters (i.e., RH and temperature) differently (Cernusak et al., 2022). The stronger correlations for $\delta^{2}H_{leaf}$ values than $\delta^{18}O_{leaf}$ values with isotopic values of the source water were likely because the $\delta^{2}H_{leaf}$ values are ultimately determined only by precipitation $\delta^{2}H$ (Sachse et al., 2012; Liu et al., 2016), whereas the $\delta^{18}O_{leaf}$ values are affected by a mixture of precipitation $\delta^{18}O$ and atmospheric factors (O_2 and CO_2) (Barbour, 2007; Cernusak et al., 2016). However, the comparative responses of both $\delta^{2}H_{leaf}$ and $\delta^{18}O_{leaf}$ values to climatic parameters were probably due to the same conditions surrounding the leaf.

The results of the cluster analysis showed that the isotope values of leaf water ($\delta^{18}O_{leaf}$ and $\delta^{2}H_{leaf}$) and twig water ($\delta^{18}O_{twig}$ and $\delta^{2}H_{twig}$) were clustered into one group, but those of soil water ($\delta^{18}O_{soil}$ and $\delta^{2}H_{soil}$) and precipitation ($\delta^{18}O_{p}$ and $\delta^{2}H_{p}$) were clustered into another (Fig. 2a). This indicates that the direct source water of $\delta^{18}O_{leaf}$ and $\delta^{2}H_{leaf}$ should be $\delta^{18}O_{twig}$ and $\delta^{2}H_{twig}$, providing the source water isotope basis for the C-G model. In the C-G model (see Equation 2), besides the source water isotopes, the equilibrium fractionation factor (ε^{+}) and atmospheric vapour enrichment (Δ_v)

depend on the temperature at the isotopic steady-state. Thus, the $\delta^{18}O_{leaf}$ and $\delta^{2}H_{leaf}$ values were predicted to be associated primarily with temperature, RH, and source water, which is consistent with the results from the cluster analysis that the $\delta^{18}O_{leaf}$ and $\delta^{2}H_{leaf}$ values were clustered with temperature (MAT and MMT) and RH (MARH; Fig. 2b). Based on the C-G model, we plotted the measured and predicted $\delta^{18}O_{leaf}$ and $\delta^{2}H_{leaf}$ values (Fig. 3a, c) and observed no significant differences between them (Fig. 3b, d). This is because our three-repeated samplings occur during the day when leaf water is generally near an isotopic steady-state when chloroplasts are mostly located near the evaporative sites (Cernusak et al., 2016). The non-steady state effects on leaf water isotopes were expected at night because of low stomatal conductance (Cernusak et al., 2005; Cuntz et al., 2002; Cernusak et al., 2016). Although the slopes of the predicted and measured $\delta^{18}O_{leaf}$ and $\delta^{2}H_{leaf}$ values were less than one, the C-G model still provides a reasonable framework for guiding the analysis of the different controls on $\delta^{18}O_{leaf}$ and $\delta^{2}H_{leaf}$ values.

4.2 Dual $\delta^{18}O$ and $\delta^{2}H$ plots of leaf water

There was a significant linear correlation between the $\delta^{18}O_{leaf}$ and $\delta^{2}H_{leaf}$ values, with remarkable clusters associated with the three months studied (Fig. 4). As is well-known, the LMWL, generated by precipitation $\delta^{18}O$ and $\delta^{2}H$ values at the local scale, serves as an important reference line for intercomparisons of different waters. Furthermore, the regression lines of the $\delta^{18}O$ and $\delta^{2}H$ values from soil water, twig water, and leaf water (Supplementary Fig. S2) suggest that the leaf water isotopes could well inherit isotopic

353 signals of source waters that originate from twig water, soil water, and ultimately
354 precipitation. The slopes and intercepts of the $\delta^{18}O$ and $\delta^{2}H$ values decreased
355 significantly from precipitation, soil water, twig water, and leaf water for each month,
356 except for soil water in May (Supplementary Fig. S2). Such patterns have been
357 observed in many previous calibration studies (Brooks et al., 2010; Evaristo et al., 2015;
358 Sprenger et al., 2016, 2017; Wang et al., 2017; Benettin et al., 2018; Barbeta et al., 2019;
359 Penna and Meerveld, 2019; Liu et al., 2021a). The slopes of the LMWLs were lower in
360 July (6.79) than in May (7.04) and September (6.85), but were not significantly different
361 (ANCOVA test: df = 0.47, $F = 2.49$, $p = 0.11 > 0.05$). This suggests that the local water
362 vapour from precipitation was derived from the same source across the seasons, but
363 was subject to different intensities of evaporation as the temperature changed
364 throughout the seasons (Li et al., 2019; Wu et al., 2019, 2021). The slopes of the $\delta^{18}O$
365 and $\delta^{2}H$ values from the soil, twig, and leaf waters were much smaller than the LMWLs
366 across the study months due to the secondary evaporation in the other water types.
367
368 In the dual isotope plot of leaf water, there were well-defined clusters of $\delta^{18}O_{leaf}$ and
369 $\delta^{2}H_{leaf}$ values across the three months: ^{18}O and ^{2}H were depleted in September, there
370 were intermediate values in July, and ^{18}O and ^{2}H were enriched in May (Fig. 4). When
371 focusing on each month, relatively higher isotopic values occurred at low elevations,
372 but lower isotopic values were present at high elevations despite there being no, or only
373 weak, correlations between the $\delta^{18}O_{leaf}$ and $\delta^{2}H_{leaf}$ values and altitude (Supplementary
374 Fig. S3). The correlations between the $\delta^{18}O_{leaf}$ and $\delta^{2}H_{leaf}$ values and altitude, and

between the $\delta^{18}O_{twig}$ and $\delta^{2}H_{twig}$ values and altitude, were not significant across the three months; however, the $\delta^{18}O_{p}$ and $\delta^{2}H_{p}$, and also the $\delta^{18}O_{soil}$ and $\delta^{2}H_{soil}$ values, were significantly correlated with altitude (Supplementary Fig. S3), indicating that besides source water (precipitation and soil water), other factors associated with plants also affect $\delta^{18}O_{leaf}$ and $\delta^{2}H_{leaf}$ values.

The dual isotope plot of $\delta^{18}O_{leaf}$ and $\delta^{2}H_{leaf}$ values shows a significant isotope line, $y = 4.52x - 50.7$ ($R^2 = 0.81$, $p < 0.01$; Fig. 4), but shallower slopes (3.53, 1.86, and 2.81 in May, July, and September, respectively) of $\delta^{18}O_{leaf}$ and $\delta^{2}H_{leaf}$ values were observed across the seasons (Supplementary Fig. S2). Such a correlation was supported by a recent study that conducted consecutive measurements of $\delta^{18}O$ and $\delta^{2}H$ values in xylem/leaf water in Switzerland and indicated that leaf water provided great potential to determine the source water of plants (Benettin et al., 2021). Our study showed remarkable clusters in the measured (Fig. 4) and the C-G model predicted (Fig. 3) $\delta^{18}O_{leaf}$ and $\delta^{2}H_{leaf}$ values across the months and the consistencies of respective $\delta^{18}O_{leaf}$ and $\delta^{2}H_{leaf}$ values with potential source water isotopes across months (Supplementary Fig. S1). These findings of temporally consistent dynamics among the water types (i.e., precipitation, soil water, twig/stem water, and leaf water) have been observed in a number of previous studies (Phillips and Ehleringer, 1995; Cernusak et al., 2005; Sprenger et al., 2016; Berry et al., 2017; Liu et al., 2021a).

The isotopic inheritance from precipitation to leaf water indicates that seasonal

variations of $\delta^{18}O_p$ and $\delta^{2}H_p$ values are the first-order control on the temporal patterns observed in leaf water. The seasonal dynamics of the $\delta^{18}O_p$ and $\delta^{2}H_p$ values reflect the combined effects of factors such as temperature, altitude, and precipitation amount, which are associated with orographic conditions, as well as sub-cloud evaporation, moisture recycling, and differences in the vapor source (Dansgaard, 1964; McGuire and McDonnell, 2007; Li et al., 2016; Penna and Meerveld, 2019; Wu et al., 2019). In this study, we used the HYSPLIT model to demonstrate the ultimate cause of the seasonal variations of $\delta^{18}O_{leaf}$ and $\delta^{2}H_{leaf}$ values; that is, the monthly dynamics of the $\delta^{18}O_p$ and $\delta^{2}H_p$ values. The monthly variations of the $\delta^{18}O_p$ and $\delta^{2}H_p$ values from the Global Network for Isotopes in Precipitation (GNIP, http://www.iaea.org/) at Xi'an station (1985-1992 AD), which is ~100 km from our study transect, were enriched in ^{18}O and ^{2}H in May relative to July and September (Fig. 5a, b). The cluster mean of the moisture transport routes from HYSPLIT (Draxler and Rolph, 2003) and the climatological 850 hPa wind vectors showed that the primary moisture sources were from western China and central Asia in May, the China-India Peninsula and Bay of Bengal, and local moisture recycling and convection (Fig. 5c, d, e). The seasonal variations in $\delta^{18}O_p$ and $\delta^{2}H_p$ values are consistently related to the onset, advancement, and retreat of the Asian summer monsoon and associated changes in the large-scale monsoon circulation (e.g., Zhang et al., 2020, 2021). As the summer monsoon starts in mid-May, the rainfall season starts in southern China; however, our study area is controlled mainly by moisture from the westerlies (Chiang et al., 2015) with relatively higher vapour, $\delta^{18}O_p$, and $\delta^{2}H_p$ values (Fig. 5c, a, b). In July, the summer monsoon reaches its strongest phase,

and the rainfall belt shifts to central and northern China, where the southerly wind brings plenty of moisture from the China-India Peninsula and the Bay of Bengal with lower vapour, $\delta^{18}O_p$, and $\delta^{2}H_p$ values (Fig. 5d, a, b). When the summer monsoon withdraws in September, the study area is controlled mainly by local moisture recycling and convection (Fig. 5e). Soil water, stored after the June-August monsoon rainfall with its lower $\delta^{18}O$ and $\delta^{2}H$ values, results in even lower $\delta^{18}O_p$ and $\delta^{2}H_p$ values in September than in July (Supplementary Fig. S1), casusing significantly lower $\delta^{18}O$ and $\delta^{2}H$ values of leaf water (Fig. 4).

4.3 Framework of controls for $\delta^{18}O$ and $\delta^{2}H$ values of leaf water

To delineate the mechanisms that control the $\delta^{18}O_{leaf}$ and $\delta^{2}H_{leaf}$ values, we used the SEMs to quantify the complex interactions among $\delta^{18}O_{leaf}$ or $\delta^{2}H_{leaf}$ values, source waters, and meteorological parameters (Fig. 6). The coefficients of determination (R^2) were 0.48 and 0.71 for the $\delta^{18}O_{leaf}$ and $\delta^{2}H_{leaf}$ values, respectively, indicating that the models explained more variance for $\delta^{2}H_{leaf}$ values than $\delta^{18}O_{leaf}$ values (Fig. 6). The SEMs showed that potential source waters (i.e., twig water, soil water, and precipitation) had stronger effects on $\delta^{2}H_{leaf}$ relative to $\delta^{18}O_{leaf}$ values, while the meteorological parameters showed weak effects on both $\delta^{18}O_{leaf}$ and $\delta^{2}H_{leaf}$ values (a little larger for $\delta^{2}H_{leaf}$ than $\delta^{18}O_{leaf}$ values). This is consistent with our above correlation analysis (Fig. 2). Surprisingly, the MMT had significant effects on $\delta^{18}O_p$ and $\delta^{2}H_p$ values, suggesting that temperature plays a key role in determining $\delta^{18}O_p$ and $\delta^{2}H_p$ values, but this finding is not discussed further here. Collectively, the SEMs also showed that source water

441 exerts the first-order control but affects $\delta^{18}O_{leaf}$ and $\delta^{2}H_{leaf}$ differently; the
442 meteorological parameters had a weak control on $\delta^{18}O_{leaf}$ and $\delta^{2}H_{leaf}$, with a more
443 substantial effect on $\delta^{2}H_{leaf}$ than $\delta^{18}O_{leaf}$ values.
444
445 A schematic representation of the controls on $\delta^{18}O_{leaf}$ and $\delta^{2}H_{leaf}$ values (respective and
446 dual) is shown in Fig. 7. It involves multiple processes associated with the
447 hydroclimatic and biochemical factors that affect $\delta^{18}O_{leaf}$ and $\delta^{2}H_{leaf}$ values. The
448 meteorological parameters (temperature, RH, and precipitation) exerted distinct effects
449 on the $\delta^{18}O$ and $\delta^{2}H$ values of the source water and, thus, on the $\delta^{18}O_{leaf}$ and $\delta^{2}H_{leaf}$
450 values, as demonstrated above by the SEM. Significant isotopic fractionation occurred
451 mainly at two key locations across the vertical soil profiles and leaf architectures from
452 precipitation to leaf water. First, an isotopic gradient across the vertical soil profile
453 appeared because of evaporation from the surface soil layers (Ehleringer et al., 1992;
454 Goldsmith et al., 2012; Evaristo et al., 2015). This evaporative isotopic fractionation
455 causes a linearly isotopic trajectory down the soil profile (Goldsmith et al., 2012;
456 Rothfuss and Javaux, 2017; Wu et al., 2018; Wang et al., 2019; Amin et al., 2020; Zhao
457 et al., 2020; Liu et al., 2021a). Second, there were significant isotopic heterogeneities
458 because of transpiration associated with the $\delta^{18}O_{leaf}$ (Helliker and Ehleringer, 2000;
459 Farquhar and Gan, 2003; Gan et al., 2003; Song et al., 2015) and $\delta^{2}H_{leaf}$ values
460 (Šantrůček et al., 2007; Liu et al., 2016; Liu et al., 2021b) within a leaf, which depends
461 substantially on veinal structures (Liu et al., 2021b). The within-leaf heterogeneity of
462 the $\delta^{18}O_{leaf}$ and $\delta^{2}H_{leaf}$ values can be explained using the *Péclet*-modified C-G model

(Gan et al., 2003; Farquhar and Gan, 2003; Cernusak et al., 2005, 2016). Collectively, the soil evaporation and leaf transpiration produce isotopic enrichment above source water (precipitation or soil water). Soil evaporation leads to an isotopic gradient across the vertical soil profile, providing water sources for plant root uptake without isotope fractionation during the process (Dawson and Ehleringer, 1991; Ehleringer and Dawson, 1992; Chen et al., 2020). During water transport between roots and leaf petioles, isotopic compositions of xylem water remain unaltered from those in soils (i.e., soil immobile water), until it reaches the leaf, which undergoes water loss (Ehleringer and Dawson, 1992). Within the leaf, transpiration leads to significant isotopic enrichment (Helliker and Ehleinger, 2000; Liu et al., 2015; Cernusak et al., 2016), which is highly dependent on meteorological parameters (e.g., temperature and relative humidity). However, the meteorological parameters varied with altitude and seasonality, yielding an isotopic water line (LWL) in the dual-isotope plot (Fig. 4). The LWL provides an important baseline for leaf-derived organic matter such as cellulose (e.g., Barbour, 2007; Lehman et al., 2017) and leaf wax (Liu et al., 2016, 2021). Overall, the LWL is controlled primarily by altitude and seasonality, as these are the main influencers of the hydroclimatic factors.

5 Conclusion

Along an elevation transect on the Chinese Loess Plateau, precipitation, soil water, twig water, and leaf water were repeatedly sampled to explore the controls on $\delta^{18}O_{leaf}$ and $\delta^{2}H_{leaf}$ values associated with meteorological parameters and source water. The effects

of meteorological parameters and source water on $\delta^{18}O_{leaf}$ and $\delta^{2}H_{leaf}$ values were different, and the dual $\delta^{18}O_{leaf}$ and $\delta^{2}H_{leaf}$ plot generated an isotopic line. We found that $\delta^{2}H_{leaf}$ values were more closely correlated with source water isotopes than $\delta^{18}O_{leaf}$ values, whereas $\delta^{18}O_{leaf}$ and $\delta^{2}H_{leaf}$ values were similarly correlated with meteorological parameters along the elevation transect. The observations suggest that plant organic isotopic proxies such as leaf wax and cellulose originating from $\delta^{18}O_{leaf}$ and $\delta^{2}H_{leaf}$ values can provide comparative climatic information on the Loess Plateau of China. Additionally, the dual-isotope analysis showed that the $\delta^{18}O_{leaf}$ and $\delta^{2}H_{leaf}$ values were closely correlated because of their similar altitudinal and seasonal responses. The first-order control on $\delta^{18}O_{leaf}$ and $\delta^{2}H_{leaf}$ values was the source water (i.e., precipitation), and the meteorological parameters had a comparable effect on both $\delta^{18}O_{leaf}$ and $\delta^{2}H_{leaf}$ values, which varied with altitude and season across the transect on the Loess Plateau. In the future, we will investigate the relationships of intersection angle θ with hydroclimatic and biochemical factors.

Competing interests

The authors declare that they have no known competing financial interests or personal relationships that could have appeared to influence the work reported in this paper.

Acknowledgment

We thank X. Cao and M. Xing for help with laboratory assistance, and Y. Cheng for the help in the field. We thank Profs. J. J. McDonnell and L. A. Cernusak for discussing

and editing the paper. We also thank Shaanxi Meteorological Bureau for supporting meteorological data along an elevation transect. This work was supported by the Chinese Academy of Sciences (XAB2019B02; XDB40000000; ZDBS-LY-DQC033; 132B61KYSB20170005) and the National Natural Science Foundation of China (42073017).

Author contribution

J.L. conceived the idea of research, and performed the data analysis. J.L., H.W., and H.Z. wrote the manuscript. L.G. and Y.Z. edited the paper. J.L. and C.J. performed the lab work. All authors contributed to discuss the results.

Data availability statement

Data related to this article can be found in Electric Annex and Mendeley Data (https://data.mendeley.com/drafts/t44wybgpr3).

References

Amin, A., Zuecco, G., Geris, J., Schwendenmann, L., McDonnell, J.J., Borga, M., and Penna, D.: Depth distribution of soil water sourced by plants at the global scale: a new direct inference approach, Ecohydrology, 13, e2177, 2020.

Allison, G., Barnes, C., and Hughes, M.: The distribution of deuterium and ^{18}O in dry soils 2. Experimental, J. Hydrol., 64, 377–397, 1983.

Barbeta, A., Jones, S. P., Clavé, L., Gimeno, T. E., Fréjaville, B., Wohl, S., and Ogée,

J.: Unexplained hydrogen isotope offsets complicate the identification and quantification of tree water sources in a riparian forest, Hydrol. Earth Syst. Sci., 23, 2129–2146, 2019.

Barbour, M. M.: Stable oxygen isotope composition of plant tissue: a review. Funct. Plant Biol., 34, 83–94, 2007.

Barbour, M. M., Farquhar, G. D., and Buckley, T. N.: Leaf water stable isotopes and water transport outside the xylem, Plant Cell Environ., 40, 914–920, 2017.

Benettin, P., Nehemy, M. F., Cernusak, L. A., Kahmen, A., and McDonnell, J. J.: On the use of leaf water to determine plant water source: A proof of concept, Hydrol. Process., DOI: 10.1002/hyp.14073, 2021.

Benettin, P., Volkmann, T. H. M., von Freyberg, J., Frentress, J., Penna, D., Dawson, T. E., and Kirchner, J. W.: Effects of climatic seasonality on the isotopic composition of evaporating soil waters, Hydrol. Earth Syst. Sci., 22, 2881–2890, 2018.

Berry, Z. C., Evaristo, J., Moore, G., Poca, M., Steppe, K., Verrot, L., Asbjornsen, H., Borma, L. S., Bretfeld, M., Herve-Fernandez, P., Seyfried, M., Schwendenmann, L., Sinacore, K., Wispelaere, L. D., and McDonnell, J.: The two water worlds hypothesis: addressing multiple working hypotheses and proposing a way forward, Ecohydrology, e1843, 2017.

Bottinga, Y., and Craig., H.: Oxygen isotope fractionation between CO_2 and water, and the isotopic composition of marine atmospheric CO_2, Earth Planet. Sci. Lett., 5, 285–295, 1969.

Bowen, G. J., and Revenaugh, J.: Interpolating the isotopic composition of modern

meteoric precipitation, Water Resour. Res., 39, 1299, 2003.

Bowen, G. J.: Isoscapes: Spatial pattern in isotopic biogeochemistry, Annu. Rev. Earth Planet. Sci., 2010, 161–187, 2010.

Bowen, G. J., and Good, S. P.: Incorporating water isoscapes in hydrological and water resource investigations, Wiley Interdiscip. Rev. Water, 2, 107–119, 2015.

Brooks, J. R., Barnard, H. R., Coulombe, R., and McDonnell, J. J.: Ecohydrologic separation of water between trees and streams in a Mediterranean climate, Nat. Geosci., 3, 100–104. 2010.

Cernusak, L. A., Farquhar, G. D., and Pate, J. S.: Environmental and physiological controls over oxygen and carbon isotope composition of Tasmanian blue gum, *Eucalyptus globulus*, Tree Physiol., 25, 129–146, 2005.

Cernusak, L. A., Barbour, M. M., Arndt, S. K., Cheesman, A. W., English, N. B., field, T. S., Helliker, B. R., Holloway-Phillips, M. M., Holtum, J. A. M., Kahmen, A., McInerney, F. A., Munksgaard, N. C., Simonin, K. A., Song, X., Stuart-Williams, H., West, J. B., and Farquhar, G. D.: Stable isotopes in leaf water of terrestrial plants. Plant Cell Environ., 39, 1087–1102, 2016.

Cernusak, L. A., Barbeta, A., Bush, R., Eichstaedt R., Ferrio, J., Flanagan, L., Gessler, A., Martín-Gómez, P., Hirl, R., Kahmen, A., Keitel., C., Lai, C., Munksgaard, N., Nelson, D., Ogée J., Roden, J., Schnyder, H., Voelker, S., Wang L., Stuart-Williams, H., Wingate, L., Yu, W., Zhao, L., Cuntz, M., 2022. Do ^{2}H and ^{18}O in leaf water reflect environmental drivers differently? New Phytologist, DOI: 10.1111/nph.18113.

Chen. Y., Helliker, B. R., Tang, X., Li, F., Zhou, Y., and Song, X.: Stem water cryogenic

573 extraction biases estimation in deuterium isotope composition of plant source water,
574 Proc. Natl. Acad. Sci., 117, 33345–33350, 2020.
575 Chiang, J. C., Fung, I. Y., Wu, C. -H., Cai, Y., Edman, J. P., Liu, Y., Day, J. A.,
576 Bhattacharya, T., Mondal, Y., and Labrousse, C. A.: Role of seasonal transitions and
577 westerly jets in East Asian paleoclimate, Quat. Sci. Rev., 108, 111–129, 2015.
578 Craig, H., and Gordon, L. I.: Deuterium and oxygen-18 variations in the ocean and the
579 marine atmosphere. In 'Proceedings of a conference on stable isotopes in
580 oceanographic studies and paleotemperatures', pp. 9–130, 1965.
581 Cuntz M., Ogée J., Farquhar G.D., Peylin P. & Cernusak L.A.: Modelling advection
582 and diffusion of water isotopologues in leaves. Plant Cell Environ. 30, 892–909, 2007.
583 Dansgaard, W.: Stable isotopes in precipitation, Tellus, 16, 436–468, 1964.
584 Dawson, T. E. and Ehleringer, J. R.: Streamside trees that do not use stream water,
585 Nature, 350, 335–337, 1991.
586 Dongmann. G., Nurnberg, H. E., Forstel, H., and Wagener, K.: On the enrichment of
587 $H_2{}^{18}O$ in the leaves of transpiring plants, Radiat. Environ. Biophys. 11, 41–52, 1974.
588 Draxler, R. R., and Rolph, G. D.: HYSPLIT (Hybrid Single-Particle Lagrangian
589 Integrated Trajectory) Model Access via NOAA ARLREADY. htmlNOAA Air
590 Resources Laboratory, http://www.arl.noaa.gov/ready/hysplit4, 2003.
591 Ehleringer, J. R. and Dawson, T. E: Water uptake by plants: perspectives from stable
592 isotope composition, Plant Cell Environ., 15, 1073–1082, 1992.
593 Ehleringer, J. R. and Dawson, T. E.: Water uptake by plants: perspectives from stable
594 isotope composition, Plant Cell Environ., 15, 1073–1082, 1992.

595 Ellsworth, P. Z., and Williams, D. G.: Hydrogen isotope fractionation during water
596 uptake by woody xerophytes, Plant Soil, 291, 93–107, 2007.
597 Evaristo J., Jasechko S., and McDonnell J. J.: Global separation of plant transpiration
598 from groundwater and streamflow, Nature, 525, 91–94, 2015.
599 Farquhar, G. D., Cernusak, L. A., and Barnes, B.: Heavy water fractionation during
600 transpiration, Plant Physiol., 143, 11–18, 2007.
601 Farquhar, G. D., and Cernusak, L. A.: On the isotopic composition of leaf water in the
602 non- steady state, Funct. Plant Biol., 32, 293–303, 2005.
603 Farquhar, G..D., and Gan, K..S.: On the progressive enrichment of the oxygen isotopic
604 composition of water along leaves, Plant Cell Environ., 26, 801–819, 2003.
605 Farquhar, G. D., and Lloyd, J.: Carbon and oxygen isotope effects in the exchange of
606 carbon dioxide between terrestrial plants and the atmosphere. In Stable Isotopes and
607 Plant Carbon–Water Relations (eds J.R. Ehleringer, A.E. Hall, & G.D. Farquhar), pp.
608 47–70. Academic Press, San Diego, 1993.
609 Gan, K.S., Wong, S.C., Yong, J.W.H., Farquhar, G.D., 2003. Evaluation of models of
610 leaf water^{18}O enrichments of spatial patterns of vein xylem, leaf water and dry matter
611 in maize leaves. Plant Cell Environ. 26, 1479–1495.
612 Goldsmith, G. R., Munoz-Villers, L. E., Holwerda, F., McDonnell, J. J., Asbjornsen, H.,
613 and Dawson, T. E.: Stable isotopes reveal linkages among ecohydrological processes in
614 a seasonally dry tropical montane cloud forest, Ecohydrology, 5, 779–790, 2012.
615 Helliker, B. R., and Ehleringer, J. R.: Establishing a grassland signature in veins: ^{18}O in
616 the leaf water of C_3 and C_4 grasses, Proc. Natl. Acad. Sci., 97, 7894–7898, 2000.

Hepp, J., Schäfer, I. K., Lanny, V., Franke, J., Blidtner, M., Rozanski, K., Glaser, B., Zech, M., Eglinton, T. I., and Zech, R.: Evaluation of bacterial glycerol dialkyl glycerol tetraether and ^{2}H-^{18}O biomarker proxies along a central European topsoil transect, Biogeosciences, 17, 741–756, 2020.

Kahmen, A., Sachse, D., Arndt, S. K., Tu, K. P., Farrington, H., Vitousek, P. M., and Dawson, T. E.: Cellulose $\delta^{18}O$ is an index of leaf-to-air vapor pressure difference (VPD) in tropical plants, Proc. Natl. Acad. Sci., 108, 1981–1986, 2011.

Leaney, F., Osmond, C., Allison, G., and Ziegler, H.: Hydrogen-isotope composition of leaf water in C_3 and C_4 plants: its relationship to the hydrogen-isotope composition of dry matter, Planta, 164, 215–220, 1985.

Lehmann, M. M., Gamarra, B., Kahmen, A., Siegwolf, R. T. W., and Saurer, M.: Oxygen isotope fractionations across individual leaf carbohydrates in grass and tree species. Plant Cell Environ., 40, 1658–1670, 2017.

Li, Z., Feng, Q., Wang, Q., Kong, Y., Cheng, A., Yong, S., Li, Y., Li, J., and Guo, X.: Contributions of local terrestrial evaporation and transpiration to precipitation using $\delta^{18}O$ and D-excess as a proxy in Shiyang inland river basin in China, Global Planet. Change, 146, 140–151, 2016.

Li, Z., Li, Z., Yu, H., Song, L., and Ma, J.: Environmental significance and zonal characteristics of stable isotope of atmospheric precipitation in arid Central Asia. Atmos. Res., 227, 24–40, 2019.

Lin, G. H., and Sternberg, L. S. L.: Hydrogen isotopic fractionation by plant roots during water uptake in coastal wetland plants. Stable Isotopic and Plant Carbon/Water

639 Relations, Academic Press, New York, pp. 497–510, 1993.
640 Liu, J., Liu, W., and An, Z.: Insight into the reasons of leaf wax $\delta D_{n\text{-}alkane}$ values between
641 grasses and woods, Sci. Bull., 60, 549–555, 2015.
642 Liu, J., Liu, W., An, Z., and Yang, H.: Different hydrogen isotope fractionations during
643 lipid formation in higher plants: Implications for paleohydrology, Sci. Report, 6, 19711,
644 2016.
645 Liu, J., Wu, H., Cheng, Y., Jin, Z., and Hu, J.: Stable isotope analysis of soil and plant
646 water in a pair of natural grassland and understory of planted forestland on the Chinese
647 Loess Plateau, Agr. Water Manage., 249, 106800, 2021a.
648 Liu, J., An, Z., and Lin, G.: Intra-leaf heterogeneities of hydrogen isotope compositions
649 in leaf water and leaf wax of monocots and dicots, Sci. Total Environ., 770, 145258,
650 2021b.
651 Liu, J.: Seasonality of the altitude effect on leaf wax n-alkane distributions, hydrogen
652 and carbon isotopes along an arid transect in the Qinling Mountains. Sci. Total Environ.,
653 778, 146272, 2021.
654 Majoube M. Fractionnement en oxygen-18 et en deuterium entre l'eau et sa vapeur.
655 Journal de Chimie et Physique 68, 1423–1436, 1971.
656 McGuire, K., and McDonnell J. J.: Stable isotope tracers in watershed hydrology, in
657 Stable Isotopes in Ecology and Environmental Science, Ecological Methods and
658 Concepts Series, pp. 334–374, 2007.
659 Munksgaard, N. C., Cheesman, A. W., English, N. B., Zwart, C., Kahmen, A., and
660 Cernusak, L. A.: Identifying drivers of leaf water and cellulose stable isotope

661 enrichment in Eucalyptus in northern Australia, Oecologia, 183, 31–43, 2017.
662 Ogée, J., Cuntz, M., Peylin, P., Bariac, T., 2007. Non-steady-state, non-uniform
663 transpiration rate and leaf anatomy effects on the progressive stable isotope enrichment
664 of leaf water along monocot leaves. Plant Cell Environ. 30, 367–387.
665 Pagani, M., Pedentchouk, N., Huber, M., Sluijs, A., Schouten, S., Brinkhuis, H., Damsté,
666 J. S. S., and Dichens, G. R.: Arctic hydrology during global warming at the
667 Palaeocene/Eocene thermal maximum, Nature, 442, 671–675, 2006.
668 Penna, D., and van Meerveld, H. J.: Spatial variability in the isotopic composition of
669 water in small catchments and its effect on hydrograph separation, WIREs Water, e1367,
670 2019.
671 Phillips, S. L., and Ehleringer, J. R.: Limited uptake of summer precipitation by big
672 tooth maple (*Acer grandidentatum* Nutt) and Gambels oak (*Quercus gambelii* Nutt),
673 Trees, 9, 214–219, 1995.
674 Plavcová, L., Hronková, M., Šimková, M., Květoň, J., Vráblová, M., Kubásek, J.,
675 Šantrůček, J.: Seasonal variation of $\delta^{18}O$ and $\delta^{2}H$ in leaf water of *Fagus sylvatica* L.
676 and related water compartments, J. Plant Physiol., 227, 56–65, 2018.
677 Poca, M., Coomans, O., Urcelay, C., Zeballos, S. R., Bodé, S., and Boecks, P.: Isotope
678 fractionation during root water uptake by *Acacia caven* is enhanced by arbuscular
679 mycorrhizas, Plant Soil, 441, 485–497, 2019.
680 Romero, I.C., Feakins, S.I., 2011. Spatial gradients in plant leaf wax D/H across a
681 coastal salt marsh in southern California. Org. Geochem. 42, 618–629.
682 Rothfuss, Y., and Javaux, M.: Reviews and syntheses: isotopic approaches to quantify

683 root water uptake: a review and comparison of methods, Biogeosciences, 14, 2199–
684 2224, 2017.
685 Sachse, D., Billault, I., Bowen, G.J., Chikaraishi, Y., Dawson, T.E., Feakins, S.J.,
686 Freeman, K.H., Magill, C.R., McInerney, F.A., van der Meer, M.T.J., Polissar, P.J.,
687 Robins, R.J., Sachs, J.P., Schmidt, H.L., Sessions, A.L., White, J.W.C., West, J.B.,
688 Kahmen, A., 2012. Molecular paleoyhydrology: interpreting the hydrogen-isotopic
689 composition of lipid biomarkers from photosynthesizing organisms. Annu. Rev. Earth
690 Planet. Sci. 40, 221–249.
691 Šantrůček, J., Květoň, J., Šetlík, J., Bulíčková, L., 2007. Spatial variation of deuterium
692 enrichment in bulk water of snowgun leaves. Plant Physiol. 143, 88–97.
693 Song, X., Loucos, K. E., Simonin, K. A., Farquhar, G. D., and Barbour, M. M.:
694 Measurements of transpiration isotopologues and leaf water to assess enrichment
695 models in cotton, New Phytol., 206, 637–646, 2015.
696 Schefuβ, E., Kuhlmann, H., Mollenhauer, G., Prange, M., and Pätzold, J.: Forcing of
697 wet phases in Southeast Africa over the past 17,000 year, Nature, 480, 22–29, 2011.
698 Sprenger, M., Leistert, H., Gimbel, K., and Weiler, M.: Illuminating hydrological
699 processes at the soil-vegetation-atmosphere interface with water stable isotopes, Rev.
700 Geophys., 54, 674–704, 2016.
701 Sprenger, M., Tetzlaff, D., and Soulsby, S.: Soil water stable isotopes reveal evaporation
702 dynamics at the soil-plant-atmosphere interface of the critical zone, Hydrol. Earth Syst.
703 Sci., 21, 3839–3858, 2017.
704 Wang, J., Fu, B., Lu, N., and Zhang, L.: Seasonal variation in water uptake patterns of

three plant species based on stable isotopes in the semi-arid Loess Plateau, Sci. Total Environ., 609, 27–37, 2017.

Wang, J., Lu, N., and Fu, B.: Inter-comparison of stable isotope mixing models for determining plant water source partitioning, Sci. Total Environ. 666, 685–693, 2019b.

Wu, H., Li, J., Li, X., He, B., Liu, J., Jiang, Z., and Zhang, C.: Contrasting response of coexisting plant's water-use patterns to experimental precipitation manipulation in an alpine grassland community of Qinghai Lake watershed, China, PLoS One, 13, e0194242, 2018.

Wu, H., Wu, J., Sakiev, K., Liu, J., Li, J., He, B., Liu, Y., and Shen, B.: Spatial and temporal variability of stable isotopes ($\delta^{18}O$ and $\delta^{2}H$) in surface waters of arid, mountainous Central Asia, Hydrol. Process. 33, 1658–1669, 2019.

Wu, H., Huang, Q., Fu, C., Song, F., Liu, J., Li, J.: Stable isotope signatures of river and lake water from Poyang Lake, China: Implications for river-lake interactions. J. Hydrol. 592, 125619, 2021.

Zhang, P., and Liu, W.: Effect of plant life form on relationship between δD values of leaf wax *n*-alkanes and altitude along Mount Taibai, China, Org. Geochem., 42, 100–107, 2010.

Zhao, L., Wang, L., Cernusak, L. A., Liu, X., Xiao, H., Zhou, M., and Zhang, S.: Significant difference in hydrogen isotope composition between xylem and tissue water in *Populus Euphratica*, Plant Cell Environ., 39, 1848–1857, 2016.

Zhao, Y., Wang, Y., He, M., Tong, Y., Zhou, J., Guo, X., Liu, J., Zhang, X.: Transference of *Robinia pseudoacacia* water-use patterns from deep to shallow soil layers during the

transition period between the dry and rainy seasons in a waterlimited region, For. Ecol. Manag., 457, 117727, 2020.

Zhang, H., Cheng, H., Cai, Y., Spötl, C., Sinha, A., Kathayat, G., Li, H.: Effect of precipitation seasonality on annual oxygen isotopic composition in the area of spring persistent rain in southeastern China and its paleoclimatic implication, Clim. Past, 16, 211–225, 2020.

Zhang, H., Zhang, X., Cai, Y., Sinha, A., Spötl, C., Baker, J., Kathayat, G., Liu, Z., Zhao, J., Jia, X., Du, W., Ning, Y., An, Z., Edwards, R.L., Cheng, H.: A data-model comparison pinpoints Holocene spatiotemporal pattern of East Asian summer monsoon, Quat. Sci. Rev., 261, 106911, 2021.

Figure captions

Fig. 1 Sample sites (red dots) and weather stations (open triangles) that distribute along vertical vegetation zones across the Mt. Taibai transect on the Chinese Loess Plateau (a). The meteorological parameters (precipitation, temperature, and RH) vary with stations along elevation transect (b). Mean annul (MAP, MAT, MARH) and montly (MMP, MMT, MMRH) precipitation, temperature, and relative humidity. The subscripts refer to the month. The vertical vegetation distribution was adopted from Liu, 2021.

Fig. 2 Heatmaps of correlations (*r*) between leaf water $\delta^{18}O$ and $\delta^{2}H$ values and potential source water $\delta^{18}O$ and $\delta^{2}H$ values (twig water, soil water, and precipitation $\delta^{18}O$ and $\delta^{2}H$ values; a), and meteorological parameters (e.g., MAP, MMP, MAT, MMT, MARH, MMRH). The hierarchical cluster analysis of the isotopes of leaf water and source water (a), and meteorologica parameters (b). The subscripts (p, soil, twig, leaf)

refer to precipitation, soil water, twig water, and leaf water. * Corrected significance at $p < 0.05$; ** corrected significance at $p < 0.01$; *** corrected significance at $p < 0.001$.

Fig. 3 Measured leaf water isotopic composition for $\delta^{18}O$ (a) and $\delta^{2}H$ (c) values against values predicted by the C-G model. Boxplots show no significant differences for $\delta^{18}O$ (b) and $\delta^{2}H$ (d) values between measured and predicted leaf water. The dotted lines show one-to-one lines.

Fig. 4 Correlation of leaf water $\delta^{18}O$ and $\delta^{2}H$ values across months and altitude. Leaf water $\delta^{18}O$ and $\delta^{2}H$ values were the higher in May, intermediate in July, and lower in September, and while within each month, those isotopic values were relatively lower at high altitudes and higher in lower altitudes.

Fig. 5 Variation of monthly mean precipitation $\delta^{18}O$ (a) and $\delta^{2}H$ (b) values at Xi'an station from Global Network of Isotopes in Precipitation (GNIP) and cluster mean of moisture transport routes using HYSPLIT model in May (c), July (d) and September (e), 2020. Background in (c-e) is the average precipitation (mm/day) and 850 hPa wind vectors (arrows, m/s) in May (c), July (d) and September (e) in 1979-2016 AD based on the database of the Global Precipitation Climatology Center (GPCC) (Becker et al., 2011) and the Modern-Era Retrospective analysis for Research and Applications (Rienecker et al., 2011).

Fig. 6 Structural equation model (SEM) of leaf water $\delta^{18}O$ (a) and $\delta^{2}H$ (b) values. The structural equation models considered all plausible pathways. Solid lines indicate significant positive (red) or negative (blue) effects, and dashed lines indicate non-significant effects. Grey lines indicate correlations between two variables. Numbers on the arrow indicate significant standardized path coefficients, proportional to the arrow width. The coefficients of determination (R^2) represent the proportion of variance explained by the model.

Fig. 7 Schematics of the respective and dual isotopes of $\delta^{18}O$ and $\delta^{2}H$ values from precipitation to leaf water, associated with physical (evaporation at soil profile and transpiration at leaf level) and biochemical processes. The dual isotopes of $\delta^{18}O$ and $\delta^{2}H$ values yield an isotopic water line, the slope of which was lower than the LMWL.

781 The intersected angle varied with hydroclimates, associated with altitude and
782 seasonality.
783
784
785
786
787
788
789
790
791
792
793
794
795
796

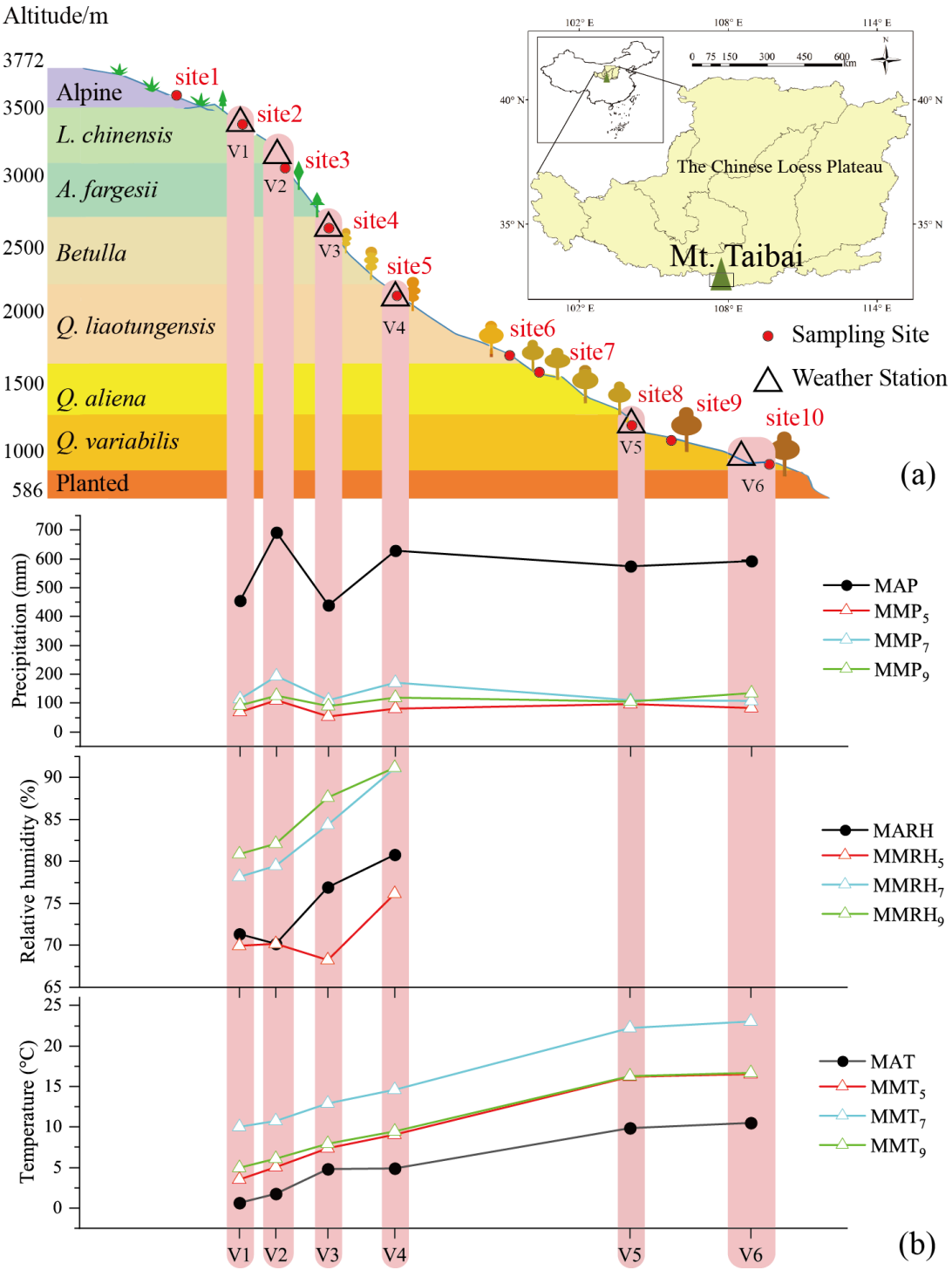
Altitude/m
3772
3500
3000
2500
2000
1500
1000
586
Alpine
L. chinensis
A. fargesii
Betulla
Q. liaotungensis
Q. aliena
Q. variabilis
Planted
site1
site2
site3
site4
site5
site6
site7
site8
site9
site10
V1
V2
V3
V4
V5
V6
102° E
108° E
114° E
40° N
35° N
0 75 150 300 450 600 km
The Chinese Loess Plateau
Mt. Taibai
Sampling Site
Weather Station
(a)
Precipitation (mm)
MAP
MMP5
MMP7
MMP9
Relative humidity (%)
MARH
MMRH5
MMRH7
MMRH9
Temperature (°C)
MAT
MMT5
MMT7
MMT9
(b)

Figure 1

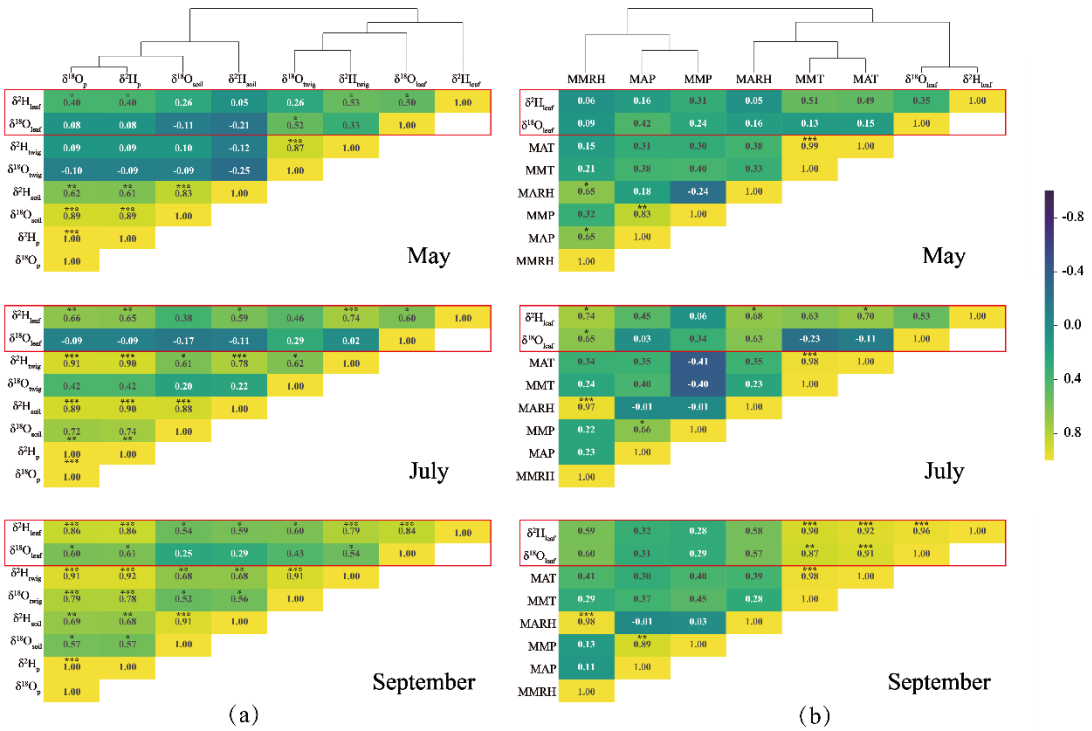

Figure 2

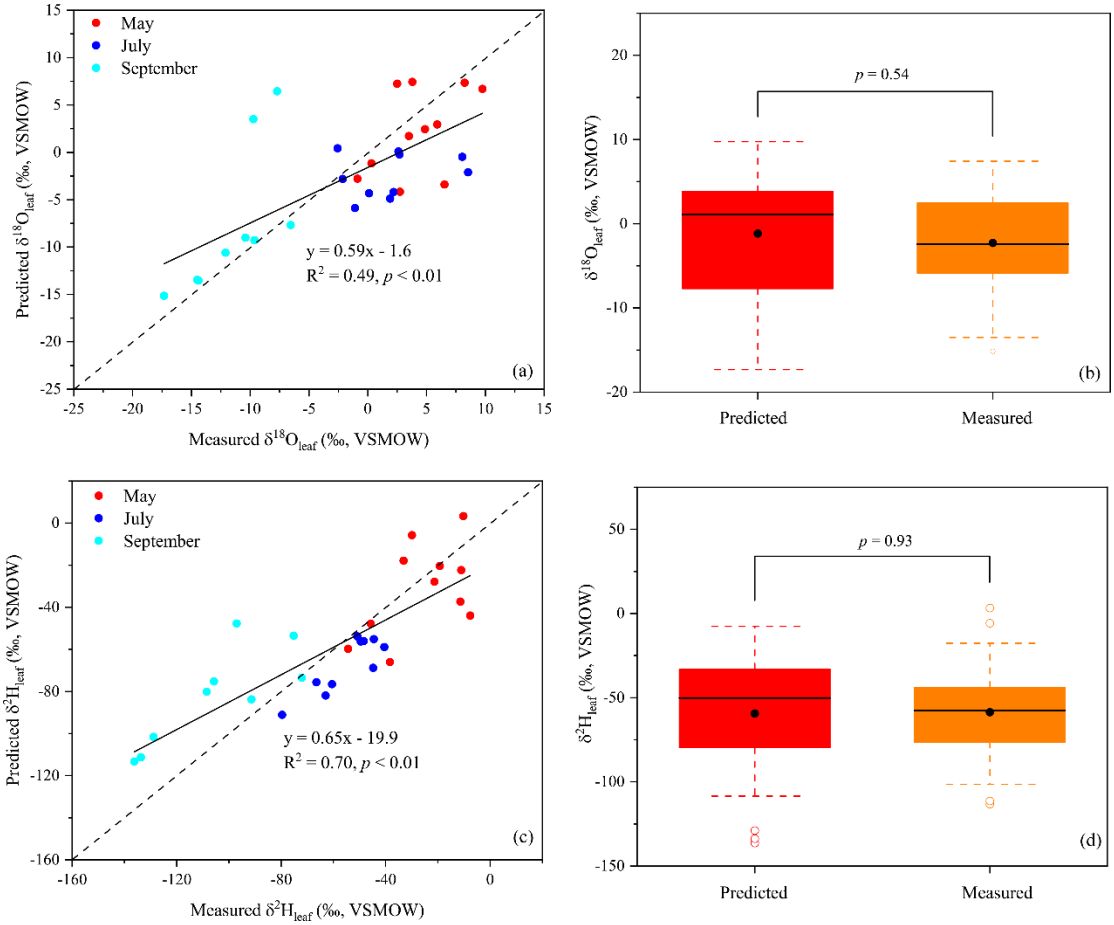

821

822 Figure 3

823

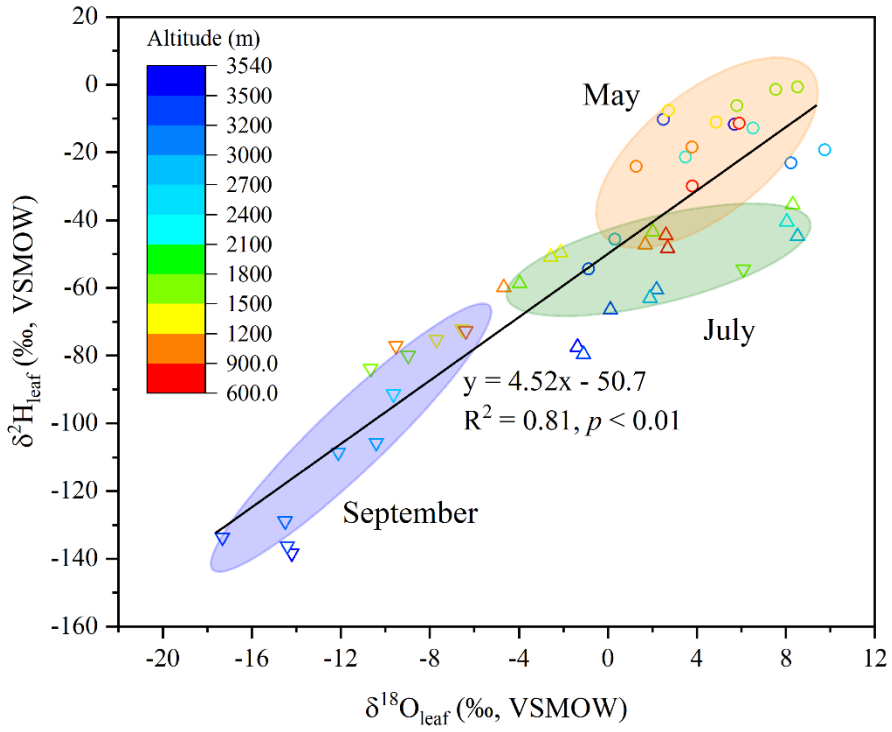

824

825 Figure -4

826

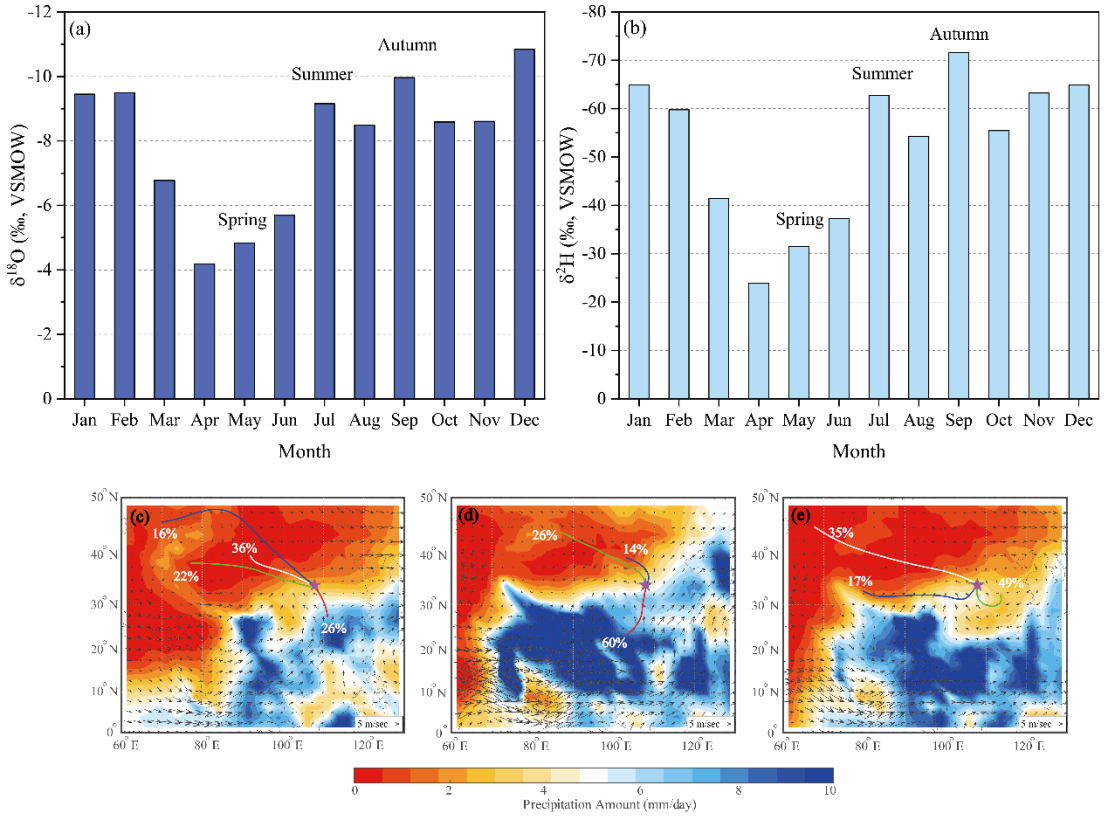

827

828 Figure -5

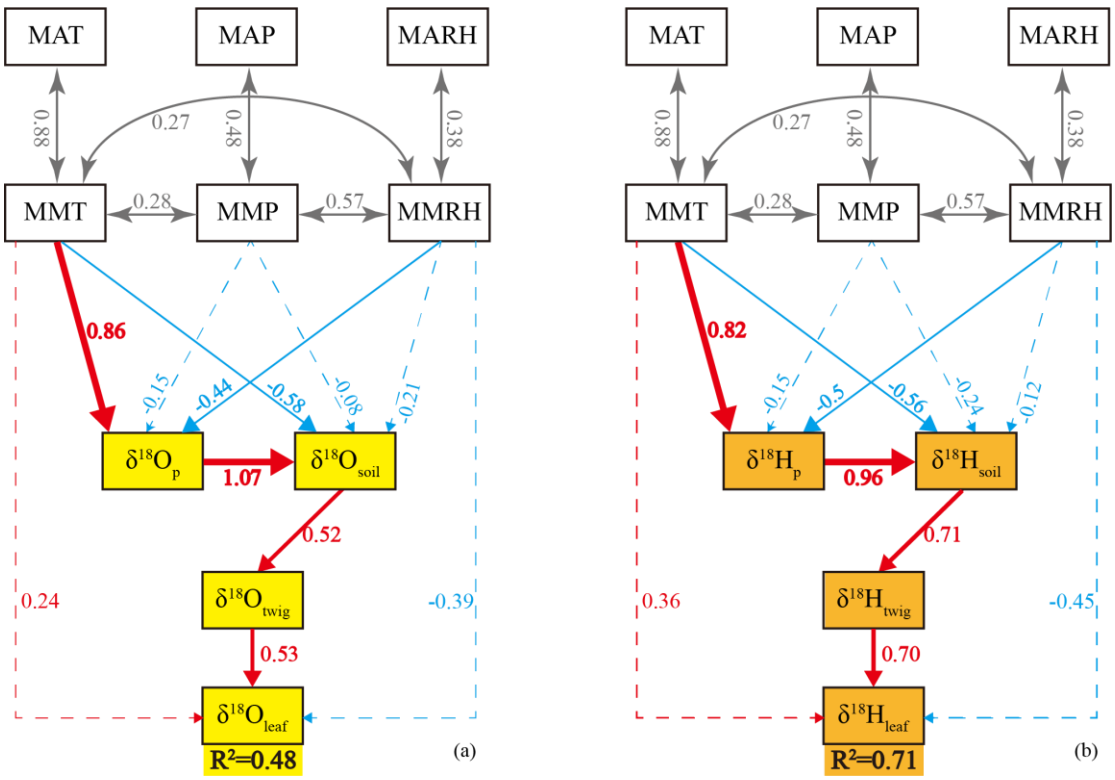

χ^2=15.7, P=0.13
CFI=0.95, GFI=0.89, RMSEA=0.11

χ^2=9.4, P=0.23
CFI=0.99, GFI=0.92, RMSEA=0.01

Figure 6

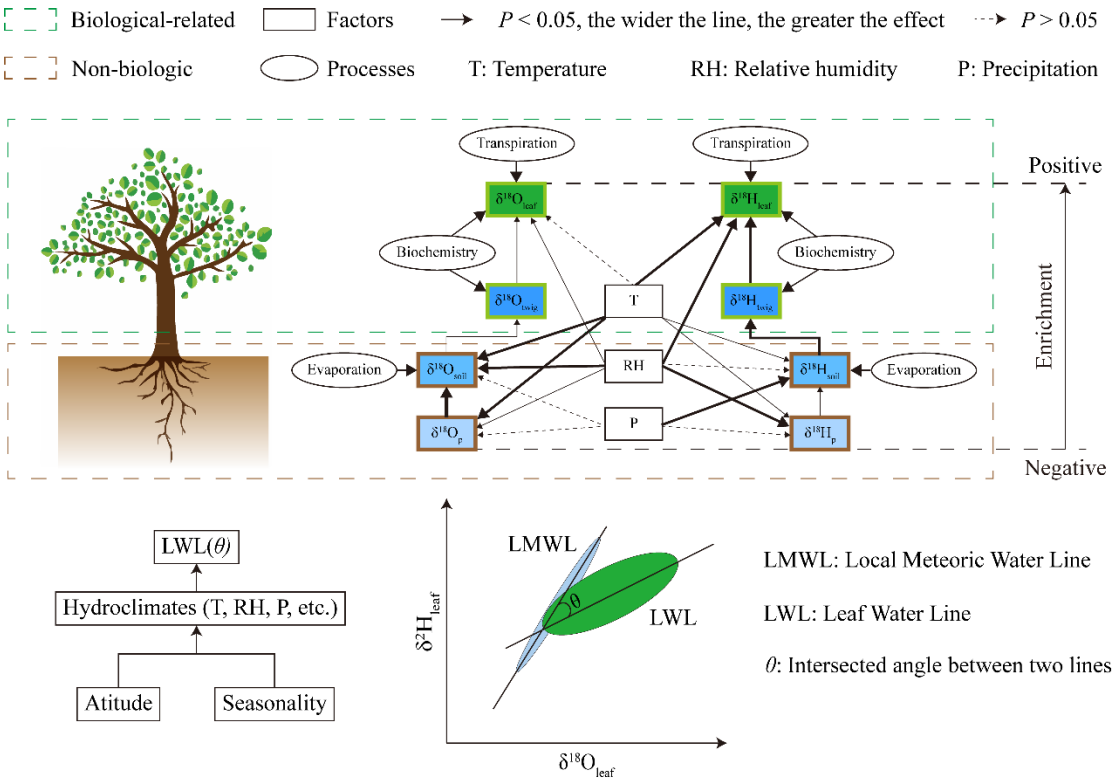

Figure 7